Renewable Energy 90 (2016) 83–94

Contents lists available at ScienceDirect

Renewable Energy

journal homepage: www.elsevier.com/locate/renene

Heat extraction of novel underground well pattern systems for geothermal energy exploitation

Peixue Jiang [a, b], Xiaolu Li [a, b], Ruina Xu [a, b, *], Fuzhen Zhang [a, b]

[a] Key Laboratory of CO_2 Utilization and Reduction Technology of Beijing, Department of Thermal Engineering, Tsinghua University, Beijing 100084, PR China
[b] Key Laboratory for Thermal Science and Power Engineering of Ministry of Education, Beijing 100084, PR China

ARTICLE INFO

Article history:
Received 4 August 2015
Received in revised form
25 November 2015
Accepted 25 December 2015
Available online 2 January 2016

Keywords:
Underground well pattern systems
Production temperature
Production pressure
Geothermal exploitation
Numerical modeling

ABSTRACT

The current Enhanced Geothermal Systems (EGS) with a fractured reservoir undergoes several practical issues, such as scaling in the wellbore, the mass flow loss into the reservoir, and the challenge in designing the placement of production wells. In this paper, novel underground well pattern systems were proposed for geothermal energy exploitation. A numerical model of two kinds well pattern systems (multi-horizontal-wells system and annular-wells system) were setup taking into account the heat exchange with the surrounding formation. The numerical model was validated by the logging data from Ordos CO_2 geological storage demonstration project, China. A comparison between the well pattern system and a fractured reservoir was conducted based on European EGS site at Groβ Schonebekc, Germany. Results showed that when the horizontal well length of well pattern system was about 10 times to the fractured reservoir, the production wellhead temperature and pressure of eight horizontal wells system with CO_2 were respectively 38.9 °C higher and 10.9 MPa higher than that of the fractured reservoir system with CO_2 after 20 years at a flow rate of 20 kg/s, an injection temperature of 20 °C and an injection pressure of 10 MPa, showing a significant application potential of the well pattern system.

1. Introduction

Under the stresses of greenhouse gas control and environmental conservation, the whole world has been increasingly attaching importance to the renewable energy. Geothermal energy, among all the types of the renewable energy, has huge potentials spread all over the earth and own advantages on the consistently stability regardless of the external weather and time. IEA (International Energy Agency) predicted that, geothermal electricity generation could get to 1400 TWh per year by 2050, contributing around 3.5% of the forecast global electricity consumption in the world for that year [1].

Geothermal fields could be utilized for heat direct use or for electrical power generation [2]. Geothermal power plants, based on high temperature hydrothermal reservoirs, are operating in at least 24 countries in the world, having a power capacity of nearly 11.0 GWe by 2010 [3], however, restricted to a few areas for the essential demands for ground water and high permeability. Enhanced Geothermal Systems (EGS), with a reservoir of low permeability, low fluid content and low hydraulic connectivity, but existing everywhere, has been proposed [2]. Up to now, some EGS demonstration projects have been operating in the world, e.g., the Fenton Hill and Desert peak projects in the United States, Rosemanowes project in UK, Soultz-sous-Forêts project in France, Hijiori project in Japan, Cooper basin project in Australia, Deep Heat Mining (DHM) projects in Switzerland, and Gross Schoenebeck project in Germany [4,5]. China also increases emphasis on the development of geothermal energy since the government has announced a target to reduce the greenhouse gas emissions at around 2030 and use non-fossil fuels for 15% of its energy structure by 2020 [4].

In EGS projects, the working fluid is pumped into reservoir through injection wells to extract the geothermal energy, enters energy conversion system on the ground or the heat use facilities from the production wells for generating electricity or heat use, and then recirculated underground. Initially the reservoir is hydraulic fractured by pressurized water to improve the permeability and to create hydraulic conductivity between the injection wells and the productions wells. Investigations on heat extraction and power

* Corresponding author. Key Laboratory of CO_2 Utilization and Reduction Technology of Beijing, Department of Thermal Engineering, Tsinghua University, Beijing 100084, PR China
E-mail address: ruinaxu@mail.tsinghua.edu.cn (R. Xu).

http://dx.doi.org/10.1016/j.renene.2015.12.062
0960-1481/

generation of EGS have been conducted by many researchers. Li and Lior [6] analyzed and compared leading geothermal power plant configurations with a geofluid temperature from 200 to 800 °C, and also analyzed the embodied energy of EGS surface power plants. Li and Lior [7] also analyzed fracturing and thermal performance of fractured reservoirs in EGS from a depth of 5 km–10 km using an improved model for flow and heat transfer. Effects of the geofluid flow direction choice, distance between fractures, fracture width, permeability, radius, and number of fractures, on reservoir heat drawdown time were obtained. Chen and Jiang [8] numerically simulated the heat extraction process of EGS with various well layouts, including the standard doublet well layout, two triplet well layouts, and a quintuplet well layout assuming the created heat reservoir could be treated as a homogeneous porous medium. Their simulation results enabled a detailed analysis on the influences of well layout on EGS heat extraction performance. Ekneligoda and Min [9] presented a nomogram solution for the evaluation of the production temperature that incorporated the mass flow rate, fracture width, fracture length, number of conductive fractures, host rock temperature, and the production time of EGS by using both an analytical and numerical model. Bujakowski et al. [10] conducted numerical modeling using TOUGH2 code to evaluate the energy performance of the prospective EGS plant operating in the Lower Triassic sedimentary formations of the Polish Lowland. Results indicated that the energy performance of the EGS plant was strongly dependent on the volume and permeability of the artificially fractured zone. Zhang et al. [11] conducted comparison of system thermodynamic performance of CO_2-EGS and water-EGS systems.

However, the Enhanced Geothermal Systems with a fractured reservoir undergoes several practical issues, such as the huge demand for water, large pressure drop through the fractured reservoir, corrosion and scaling in the wellbores due to the direct contact of the working fluid with the reservoir rock surface, the mass flow loss into the reservoir and the challenge of choosing production well drilling location due to the difficulty in controlling the fracture channels. For instance, in Rosemanowes project in UK, when the injection rate was 5 l/s, the return from the production well was 4 l/s; when 24 l/s was injected, only 15 l/s was produced [5]. In Hijiori project, the production wells had to be cleaned-out due to scaling problems and the flow rate loss was as high as 45% during long-term test from 2000 to 2002. The test was finally stopped due to the drop in production temperature which was larger than the numerically predicted temperature drop [5]. Therefore, an ideal geothermal exploitation method should have a comprehensive advantage on generating efficiency, pressure drop, environmental impact, cost, and flow rate loss. Currently, the field-scale heat extraction efficiency and generating efficiency can merely be obtained through simulation tools. However, the heat transfer models in the complex subsurface structures were still insufficient [4], and no EGS reservoir has been operated for a sufficient period of time to provide the required data to validate a simulation model [2]. This brings more uncertainty on EGS with fractured reservoir when the fractured channels lead to uncertain flow and reservoir behavior under long-term energy extraction.

In this context, some researchers proposed new subsurface heat exchangers to improve the comprehensive performance of the heat extraction system. Alimonti and Soldo [12] analyzed the possibility to implement a wellbore heat exchanger on one of the largest European oil fields: the Villafortuna Trecate oilfield and demonstrated the importance to consider the change of fluid properties inside the exchanger. Galgaro et al. [13] analyzed the feasibility and sustainability of borehole heat exchangers in shallow geothermal areas which circulated a working fluid in a closed-loop of pipes installed vertically in a deep well and released the heat to buildings. It is found that an array of 4 heat-exchangers 240 m deep provided enough thermal energy to the building. Yekoladio et al. [14] designed and optimized a downhole coaxial heat exchanger employed in an Enhanced Geothermal Systems where cold water was injected from the annulus and produced from the inner tube, to maximize the cycle power output. Dehkordi et al. [15] found that in downhole heat exchangers, proximity of the pipes to the borehole wall was more important than the pipe separation in reducing the total borehole resistance. Hence, they proposed and numerically modeled a tight borehole design with little spacing between the down-hole pipes and the borehole wall. Finsterle et al. [16] used numerical simulations to explore the potential of injecting the fluid from micro-hole arrays rather than a few conventionally drilled wells to increase the heat extraction efficiency and sustainability of EGS. Results showed that micro-hole arrays provided pathway to a larger reservoir thus increasing the heat recovery factor; more importantly, the risk of preferential flow and early thermal breakthrough was reduced in microhole-array-based EGS. Jeanloz and Stone [17] discussed a closed wellbore pattern system where the working fluid flowed through wholly drilled heat exchangers. It was found from a simple heat transfer calculation that for a reservoir with the initial temperature of 250 °C, assuming water production temperature to be 150 °C (where the inlet temperature was 50 °C) after 10 years' operation, the heat exchanger should have a total length of about 2.5 km with the diameter of 1.3×10^{-2} m in order to still produce 1 MW thermal power after 10 years. Furthermore, after 40 years' operation, the thermal power produced would only have decreased by 10% to 0.9 MW. The underground closed-cycle heat exchanger system, as one of the fifteen geothermal power generation projects supported by the German government, was in the charge of Prof. Wolff from Berlin Institute of Technology [18]. The underground system included two vertical wells with the depth of 3–5 km per well and one horizontal well in which the working fluid was circulated and heated by the reservoir. On the ground, Organic-Rankine-Cycle (ORC) was used for electricity generation. Wolff stated that the underground closed-cycle heat exchange system, compared to EGS with fractured reservoirs, had advantages on the non-decreasing flow rate of the working fluid, little contamination on the reservoir, low cost of system maintenance, and long lifetime. With one horizontal well, the reservoir near the pipe center was cooled dramatically; hence, Wolff suggested to consider multi-horizontal-wells system [18]. However, based on the concept of the underground closed-cycle heat exchanger system, very few quantitative system analysis and simulation about the heat extraction performance especially with the multi horizontal wells were conducted.

In this paper, novel underground well pattern systems, replacing fracturing technology with horizontal wells technology, were proposed for geothermal energy exploitation. Different from the already proposed underground closed-cycle heat exchange system [17,18], the proposed underground well pattern systems in this paper contained multiple horizontal wells with the distance between each wells carefully designed to avoid the thermal breakthrough, or contained annular wells where the injection and production wellhead were close to each other to reduce the pressure loss in the transport pipelines on the ground. The proposed well pattern systems had dramatic advantages in solving scaling problem due to the flow inside of the wellbores, precisely controlling the flow direction and mass flow rate without loss, as well as decreasing the pressure drop from the injection well to the production well which increased the thermal efficiency. With greenhouse gas control gaining increasing attention, CO_2 can be sequestered in deep or shallow aquifers [19–21], be used to enhance CH_4 recovery [22] and to extract geothermal energy as the working fluid in EGS [23]. For EGS with CO_2 as the working fluid,

CO_2 directly entered the turbine for electricity generation from the production wellhead, different from EGS with water as the working fluid where water firstly entered the evaporator to transfer the extracted heat to the working fluid for ORC. Scaling problem in the turbine in EGS with CO_2 as the working fluid severely affected the long-term operation of CO_2 turbine, and the proposed underground well pattern systems were beneficial for CO_2 system in solving scaling problem. A numerical model of the presented well pattern was setup in this paper, taking into account the real thermal properties of working fluid, the placement and configuration of injection wells, horizontal wells and production wells, and the heat exchange with the surrounding formation. The temperature and pressure profiles in the wellbores in different designs at different production mass flow rates and injection temperatures were predicted. A comparison of the system with a fractured reservoir and the well pattern systems with water or CO_2 as the working fluid was conducted based on the geological conditions at the European EGS site at Groβ Schonebekc, Germany.

2. Novel underground well pattern systems

With the development of the advanced drilling technology, drilling a vertical or inclined well to the depth of around 4000 m have been technologically mature [24]. Horizontal drilling technology also develops rapidly, e.g., the common horizontal wells were about 1000 m long and the longest horizontal well was 1630 m by 1994 [25], and Maersk Oil Qatar completed drilling the world-record longest well in May 2008 offshore Qatar including a horizontal section measuring 10.9 km [26]. Moreover, the advances in drilling technology for slim holes (bores less than 165 mm diameter), micro holes (bores less than 102 mm diameter), and ultra-slim diameter wells (bores between 25 and 74 mm diameter) [27–29] offer the feasibility to design different well configurations for optimally extracting the geothermal energy at minimal cost using underground well pattern systems.

Two novel underground well pattern systems were proposed as shown in Fig. 1 (a) and (c) in which the vertical wells and horizontal wells were connected with inclined wells. For the convenience of simulation and analysis, the designed systems were simplified to Fig. 1 (b) and (d) for calculation. The first system consisted of four injection wells at four vertexes of a rectangular, eight horizontal wells pointing to the same direction, and one production well. The working fluid was pumped into the injection well and flows out of the production well all along in the tubing without contact with surrounding rocks. The production mass flow rate was four times of the injection mass flow rate in a single injection well. All produced heated working fluid entered the power generation system on the ground, flowed separately to the target injection wellhead through transport pipelines, and was injected into the wellbore to constitute a circulation loop. The second system was composed of four symmetric annular wells. Each annular well served as a completed channel in which the working fluid was injected and produced. The injection and production wellhead was relatively close to each other to reduce the pressure drop through transport pipelines after the power generation system, and insulation measures should be taken for the upper production well to eliminate the heat transfer between the injection and production parts. The generation power and generation efficiency after the operating time of 30 years, which are determined by the injection and production temperature, pressure and mass flow rate, are significantly influenced by the layout of the well pattern in a specific geothermal reservoir and within a certain budget. Particularly, the distances between different parts of the channels should be discreetly designed to avoid the thermal break-through of the rocks between them.

Some evolving drilling technologies, such as expandable tubular casing, drilling-with-casing, well-design changes involving the use of smaller increments in casing diameters with depth can potentially reduce the cost of drilling wells [2]. For the longer term, some revolutionary drilling technology including hydrothermal flame spallation and fusion drilling [30], chemically enhanced drilling [31] and metal shot abrasive-assisted drilling [32] may lead to a revolutionary development of these proposed ground well pattern systems. Some methods of heat transfer enhancement, for example, replacing straight tube with serpentine tube as experimentally studied by Xu et al. [33], may be the next step to improve the proposed well pattern systems.

3. Numerical approaches for underground heat transfer and ground generation performance

3.1. Physical models

For a specific geothermal reservoir with 20 °C at the surface and 250 °C at the depth of 4000 m, the proposed typical layout and configurations of multi-horizontal-wells system and annular-wells system were as shown in Fig. 2, which were taken as base cases to quantitatively investigate the heat extraction performance of these systems. Seasoning effect on ground temperature was not considered in the simulation because seasoning effect only led to temperature variations in shallow rock layers with a depth of less than 30 m [34], and the constant temperature layer, from the depth of 30 m to the depth of 4000 in the proposed systems, contributed the vast majority of heat exchange with the working fluid.

For multi-horizontal-wells system (system 1), the working fluid was injected into the reservoir at a certain wellhead temperature and an injection rate of 10 or 20 kg/s for single injection well, and produced at a total rate of 40 or 80 kg/s. The required injection pressure at the wellhead to maintain a stable circulation could be calculated when the pressure at the production wellhead was set to 5 MPa. After flowing to the depth of 4000 m, the working fluid entered a distributary horizontal well with a length of 4000 m, through which the working fluid was heated by the surrounding rocks. Along the production well from the depth of 4000 m to the ground surface, the working fluid would undergo a drop in temperature due to its expansion and the decreasing surrounding temperature. The velocity of the working fluid in different parts of the system was designed to be similar to each other, which associated with a stable circulation system. Therefore, the diameter of each tubing was determined by the flow rate distribution. The injection well, horizontal well, production well below the depth of 4000 m and production well above the depth of 4000 m had diameters of 108 mm, 76.4 mm, 152.8 mm and 216 mm respectively. An annular rock formation was set around each wellbore to provide with the geothermal energy. The distance between the shallower and deeper horizontal wells is a key parameter requiring optimization to guarantee a continuous heat source and avoid the thermal break-through of the rocks. After several trials, the distance of 200 m between horizontal wells was adopted in this system and correspondingly, the total thickness of the annular rock around the wellbore was 100 m. The outer boundary of the rocks was maintained at a linear temperature distribution with depth corresponding to the geothermal gradient, assuming uninfluenced by the circulated fluid. The feasibility to use this boundary condition and to design this distance will be discussed based on the following results.

As shown in Fig. 2 (b), the production flow rate for a single annular well was 10 or 20 kg/s and the diameter of all the tubings was 76.4 mm for the annular-wells system. The working fluid was firstly injected into a vertical wellbore with a depth of 500 m and then into an inclined wellbore to the depth of 4000 m. An annular

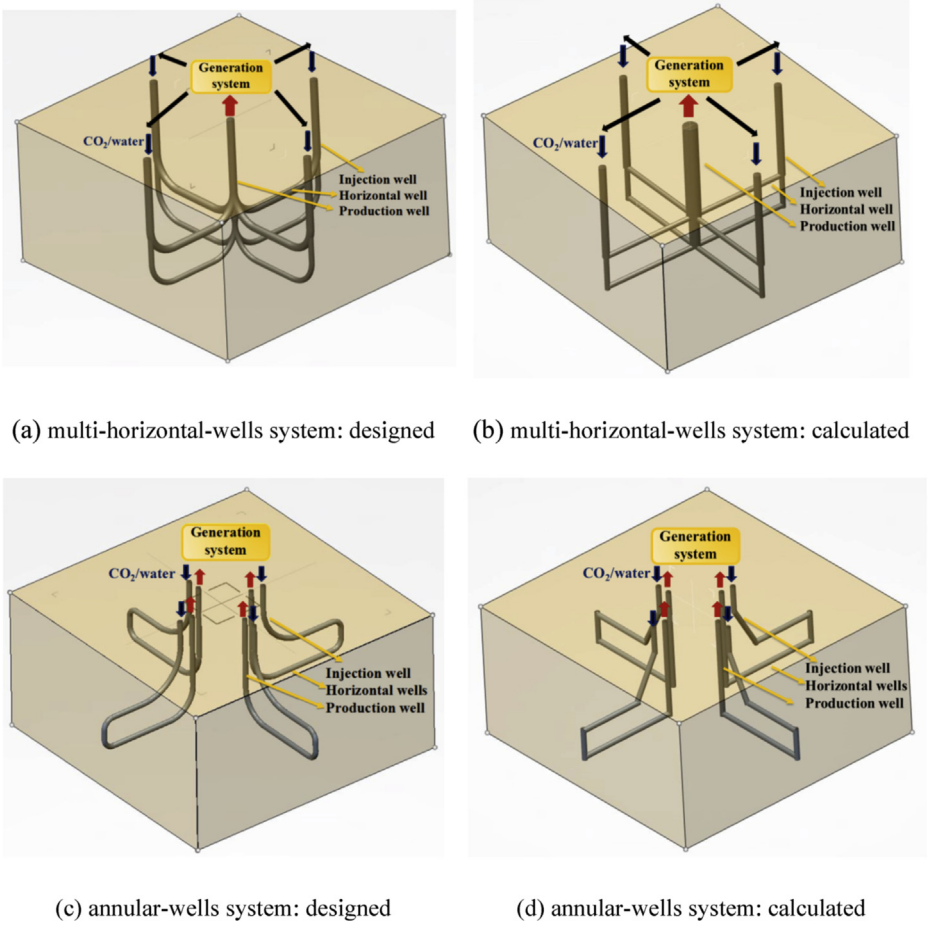

Fig. 1. Two proposed novel underground well pattern systems: (a) (c) designed systems, (b) (d) simplified models for calculation.

rock formation with a thickness of 100 m was also set around each wellbore for calculating the radial heat transfer. The injection and production wellheads just had a very small distance. Therefore, the thermally insulation was adopted to avoid the heat exchange between the injection and production wells and to eliminate the heat loss to the rocks around the tubing walls from the ground to the depth of 2250 m.

There was a layer of tubing wall outside the tubing, with a thickness of 20 mm, heat capacity of 500 J/kg·K, heat conductivity of 31.15 W/m K, and density of 7700 kg/m^3. The annular rock, with a total thickness of 100 m, was divided into 139 layers with thicknesses from 20 mm to 2 m to capture the transient radial heat transfer. The heat capacity, heat conductivity and density of the rock are 700 J/kg K, 3.9 W/m K, and 2240 kg/m^3 respectively.

3.2. Governing equations for underground flow and heat transfer

The underground flow and heat transfer were simulated using the commercial dynamic multiphase model OLGA 7.0.0. OLGA is utilized widely in oil and gas industry to simulate multiphase flow and heat transfer in the networks of wells, pipelines and process equipment, using a finite element method for discretization of continuity, momentum and energy equations with a semi-implicit time integration implemented [35]. The conservation equations are one-dimensional along the flow direction with the assumption of the uniform physical quantities in the cross section vertical to the flow direction, while the heat transfer between the surrounding rocks and the fluid in the wellbore in the radial direction can be calculated. During the steady operation of these systems, there is only liquid phase and supercritical state of the working fluid along the wellbore. However, during transient operations such as the start-up of the injection at very beginning and the shut-in of the well due to maintenance or other reasons, liquid/gas phase change may occur in the wellbore as analyzed by Li et al. [36]. The governing equations of single-phase flow in one-dimensional along the wellbore and heat transfer with the surrounding rocks were used as follows [37]:

Mass conservation equation:

$$\frac{\partial}{\partial t}(\rho) = -\frac{1}{A}\frac{\partial}{\partial z}(A\rho v) \tag{1}$$

where t is time, ρ is density, A is pipe cross-sectional area, z is the coordinate of flow direction, and v is velocity.

Momentum conservation equation:

$$\frac{\partial}{\partial t}(\rho v) = -\left(\frac{\partial p}{\partial z}\right) - \frac{1}{A}\frac{\partial}{\partial z}\left(A\rho v^2\right) - \lambda\frac{1}{2}\rho|v|v\frac{S}{4A} + \rho g\cos\alpha \tag{2}$$

where p is pressure, λ is wall friction factor, S is wet perimeter, g is gravitational acceleration, and α is pipe inclination with the vertical.

Energy conservation equation:

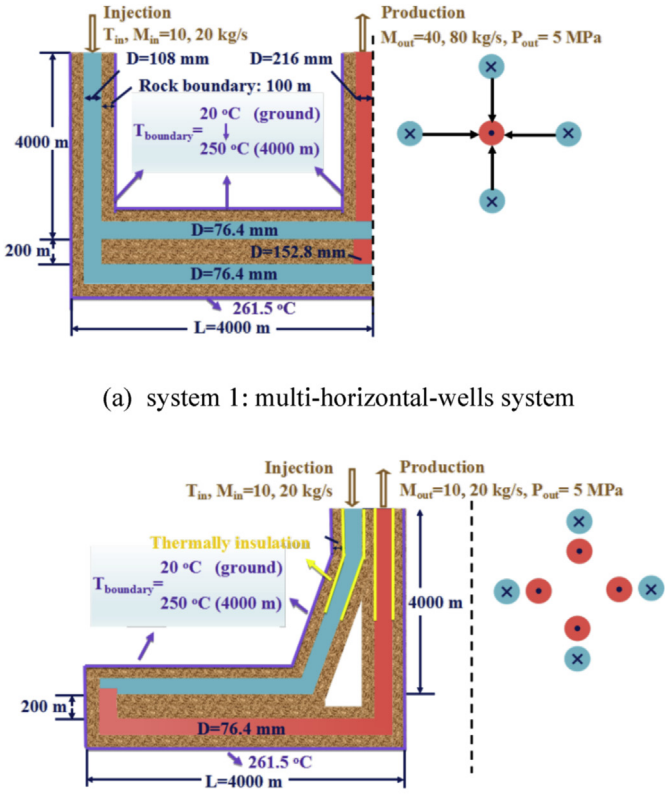

Fig. 2. Schematic diagram of geothermal well pattern systems.

$$\frac{\partial}{\partial t}\left[m\left(E+\frac{1}{2}v^2+gh\right)\right]=-\frac{\partial}{\partial z}\left[mv\left(H+\frac{1}{2}v^2+gh\right)\right]+H_S+Q \tag{3}$$

where m is mass, E is internal energy per unit mass, h is elevation, H is enthalpy per unit mass, H_S is enthalpy from mass sources, and Q is heat transfer from the rock formation.

Inside the tubing wall and the rock formation, there is only one mechanism of heat transfer, unsteady heat conduction. Therefore, in the interior of the solid wall and the rock formation, only the energy conservation with transient heat conduction in radial direction was solved using the following equation [35]:

$$\rho_w c_{pw}\frac{\partial T_w}{\partial t}=\frac{1}{r}\frac{\partial}{\partial r}\left(k_w r\frac{\partial T_w}{\partial r}\right) \tag{4}$$

where subscript w represents wall layer, c_p is specific heat capacity, T is temperature, r is radial coordinate, and k is heat conductivity.

A single component model was used in OLGA to accurately address the properties of single pure CO_2 or pure water. The SW equation was applied to calculate the density and the specific heat of CO_2 [38], while the K.S.P equation was used for calculating the viscosity and thermal conductivity of CO_2 [39]. The equations used to calculate the water properties were taken from Cooper and Dooley [40].

3.3. Boundary conditions and initial conditions

For underground system, every injection wellhead was set to have a mass flow rate of 20 kg/s or 10 kg/s and an assumed injection temperature. The production wellhead was set to a pressure of 5 MPa. The outer boundary of the annular rocks was maintained at a linear temperature distribution with depth corresponding to the geothermal gradient, with 20 °C at surface and 250 °C at 4000 m depth. A temperature distribution corresponding to this geothermal gradient in the tubing and rocks and a pressure distribution determined by the hydrostatic pressure of the working fluid in the tubing were set as the initial conditions for the transient calculations. All the transient calculations were performed till 30 years with the time step from 1 s to 1 day.

4. Results and discussions

4.1. Model validation with well log data of a CO_2 injection well

The accuracy of modeling the proposed well pattern systems was dependent on the accuracy of modeling the flow and heat transfer in the wellbores. In this section, a model using the same methods as introduced in Section 3.2 was developed to compare with the two-dimensional radial numerical model proposed by Jiang et al. [19] according to the CO_2 injection well configuration and the injection parameters in Ordos CCS project in China. The 2D radial model using CFD software FLUENT has been validated showing great consistency (to under 10%) with the well log data [19]. In the developed model, CO_2 was injected into a wellbore at 0 °C and a mass flow rate of 0.9 kg/s, and with a depth of 1500 m. The annulus was filled with water, and the surrounding rock boundary at a radial distance of 1000 m was at geothermal temperature of 13 °C at the ground surface and 56 °C at a depth of 1500 m. The thermal properties of rock were the same as those of the 2D radial model, and the properties of annular water were held constant with a specific heat capacity of 4182 J/kg K, density of 998.2 kg/m^3, and thermal conductivity of 0.6 W/m K. The calculated temperature distribution was also compared to the analytical solution presented by Hasan and Kabir [41]:

$$T_f=T_{ei}-\frac{1-e^{-zL_R}}{L_R}\left(g_G\sin\alpha+\phi-\frac{g\sin\alpha}{c_p}\right)+e^{-zL_R}\left(T_{fwh}-T_{es}\right) \tag{5}$$

Fig. 3 illustrated that after 10 days of pseudo steady-state

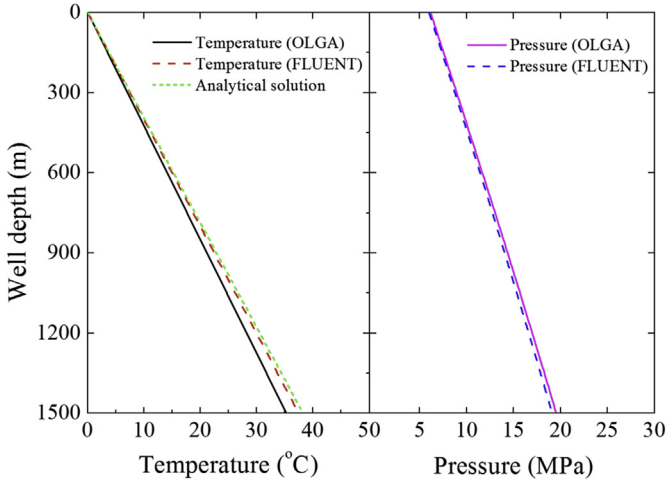

Fig. 3. Comparison of simulated CO_2 temperature profile and CO_2 pressure profile in the wellbore after 10 days injection time using FLUENT model, OLGA model, or analytical solution.

injection, the bottomhole temperature at the depth of 1500 m calculated by OLGA model was 35.2 °C, 2.2 °C lower than that calculated by FLUENT 2D radial model and 3 °C lower than the result from the analytical solution [41]. The bottomhole pressure calculated using OLGA was 19.5 MPa, 0.4 MPa larger than that calculated using FLUENT. These differences were acceptable and the following modeling was implemented using OLGA considering the computational efficiency.

4.2. Performance of heat extraction of multi-horizontal-wells system

Water was adopted as the working fluid in the analysis in this section as water was still the most common working fluid for geothermal exploitation currently. During the initial operation of the geothermal system, water extracted the maximum heat from the hot rocks, and with the rock gradually cooled by the injected water, the temperature at the production wellhead also decreased with time. With the injection temperature of 70 °C and production flow rate of 80 kg/s in the multi-horizontal-wells system shown in Fig. 4 (a), the temperature of water increased from the injection temperature of 70 °C–86 °C in the injection well and increased more significantly from 86 °C to 141 °C in the shallower horizontal well at the operation time of 1 year (Fig. 4 (a)). The temperature increase of water was focused on the horizontal well due to the consistent high temperature around and also due to the half mass flow rate in the horizontal well compared to the injection well. In the production well, water temperature decreased slightly from 147.2 °C to 143.7 °C at 1 year due to the gradually decreasing surrounding temperature. As the operation time increasing, water temperature in the wellbore approached stable condition, increasing from 70 °C to 130 °C along the whole wellbore.

Along the whole wellbore, the frictional pressure loss was a continuing factor to reduce the production pressure compared to the injection pressure. However, the hydrostatic pressure due to gravity along the injection well and the production well, although with the opposite direction, could not be counteracted because of the different density of the fluid at different temperatures. The above two factors, along with the compressibility of the fluid, could lead to the different relationship between the injection pressure and the production pressure. In the case shown in Fig. 4, the injection pressure was 6.7 MPa at 30 years, higher than the production pressure of 5 MPa.

To illustrate the interactions between the injected water and the surrounding rocks, temperature distributions of water in the tubing and different rock layers along the wellbore length in the deeper horizontal well at the operation time of 30 years were shown in Fig. 4 (b). The rock layers with distances to the wellbore axis of 0.1 m, 1 m, 10 m, 30 m, 50 m, 80 m and 90 m had been cooled from the initial temperature of 261.5 °C–110 °C, 155 °C, 212 °C, 238 °C, 249 °C, 255 °C and 260 °C respectively at the inlet of the deeper horizontal well at 30 years. With the decreasing gradient of the temperature in the further rocks from the wellbore, the temperature of rocks at a distance of 96 m and 100 m was still the initial temperature of 261.5 °C, which indicated that the influence of the injected water had not propagated to the rock boundary at the distance of 100 m and could be a verification of the availability of the rock boundary and the distance between each wellbore.

4.3. Performance of heat extraction of annular-wells system

For system 2, the production temperatures of water were 149.2 °C, 137.8 °C and 134.1 °C respectively after the operation time of 1 year, 10 years and 30 years with the injection temperature of 70 °C and production flow rate of 80 kg/s as shown in Fig. 5 (a). The injection pressure reached to 7.9 MPa after 30 years. It could be found from Fig. 5 (b) that the temperature of rocks at distances of 96 m and 100 m were also not influenced by the injected water.

System 1 and 2 were operated at different injection temperatures for the production mass flow rate of 40 kg/s and 80 kg/s to investigate the influence of the operational parameters on the performance of heat extraction. As shown in Fig. 6, the production temperature at the production wellhead decreased very slowly after the operation of 30 years. It was easy to understand that, with the smaller production flow rate of 40 kg/s and the higher injection temperature of 70 °C, the production temperature was higher. The practical generating power and generating efficiency were a comprehensive outcome from all the operation parameters. Table 1 showed the detailed injection pressure and production temperature for each scenario after 30 years. It could be found that the production temperature was 113.0 °C at the injection temperature of 40 °C and the output flow rate of 80 kg/s, only 17.0 °C lower than the production temperature at the injection temperature of 70 °C and the same flow rate. The narrowing difference between the production temperatures compared to the difference between the injection temperatures was due to larger temperature difference between water and the surrounding rocks at lower injection temperature which led to more heat extraction. One of the benefits of the smaller production flow rate was the smaller frictional pressure loss along the whole wellbores which resulted in a smaller injection pressure when the production pressure was set to 5 MPa. The injection pressures with flow rate of 40 kg/s were 2.8 MPa and 2.9 MPa respectively for the injection temperatures of 40 °C and 70 °C in system 1. These injection pressures were even lower than the production pressures and could provide with the self-driven force for the consistent circulation. However, with a larger flow rate of 80 kg/s, the injection pressure was higher than the production pressure and thus required the extra pump power to realize the high-pressure injection. System 2 was better than system 1 for the higher production temperature at the same injection temperature and mass flow rate (Table 1) and for the smaller pressure drop from the production wellhead to the injection wellhead as the closer position.

4.4. Comparison between the fractured reservoir and the well pattern systems

To better illustrate the potential advantages of the underground well pattern systems for geothermal energy exploitation, a comparison of the EGS with a fractured reservoir and the well pattern systems was conducted based on the geological conditions at the European EGS site at Groβ Schonebekc, Germany. The CFD simulation results of EGS with a fractured reservoir with CO_2 as the working fluid from Luo et al. [42] were adopted as the comparison object. The geological conditions, well configurations and injection parameters for EGS model of Luo et al. [42,43] and for calculation of well pattern systems were shown in Table 2.

The site at Groβ Schonebekc had a geothermal gradient of 3.5 °C/100 m, and the temperatures of ground surface, depth of 4050 m and depth of 4250 m were 8 °C, 149.75 °C and 156.75 °C, respectively. The density, thermal conductivity and specific heat capacity of the reservoir rock at the site were 2650 kg/m^3, 2.9 W/m·K and 905.7 J/kg·K, respectively. As shown in Fig. 7 (a), the existing Enhanced Geothermal Systems at Groβ Schonebekc consist of one injection well, one production well and a fractured reservoir. The injection wellbore and production wellbore had a depth of 4250 m with a diameter of 230 mm, and the distance between two wells was 424.2 m which was the length of the fractured reservoir. In the proposed well pattern systems with one or eight horizontal wells as shown in Fig. 7(b) and (c), the length of single horizontal well, or

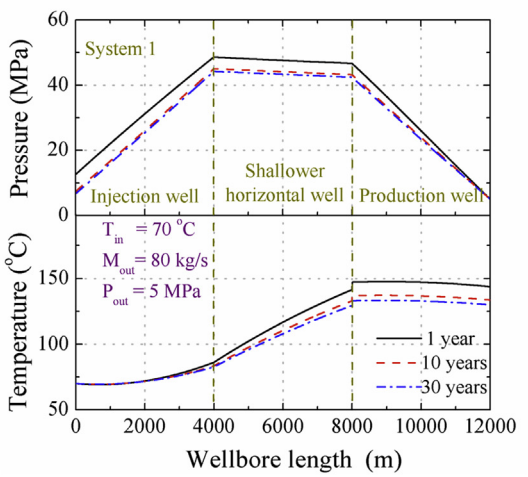

(a) pressure and temperature distributions of water in the tubing along the wellbore length in the injection well, shallower horizontal well and production well at the operation times of 1 year, 10 years and 30 years

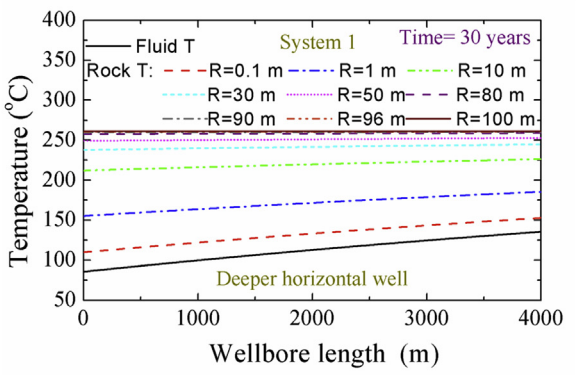

(b) temperature distributions of water in the tubing, rock with a radial distance to the wellbore axis of 0.1 m, 1 m, 10 m, 30 m, 50 m, 80 m, 90 m, 96 m and 100 m along the wellbore length in the deeper horizontal well of system 1 at the operation time of 30 years

Fig. 4. Temperature and pressure distributions along the wellbore length with the injection temperature of 70 °C, production flow rate of 80 kg/s and production pressure of 5 MPa in multi-horizontal-wells system.

the distance between the injection and production well was designed to be 4000 m, much longer than the fractured reservoir due to the larger velocity in the horizontal well than that in the fractured reservoir in order to obtain the comparable heat extraction rate. It should be noted that the costs of hydraulic stimulation of the reservoir and drilling wells are dependent on several parameters such as the initial reservoir temperature, wellbore length and fracture dimensions. In the study of the University of Pittsburgh in 2011 [44], total cost for drilling the horizontal part of a Marcellus Shale well with a length of 1524 m in Southwestern Pennsylvania was about $1.2 million, and the hydraulic fracturing of the reservoir cost about $2.5 million, assuming 15 fracturing stages. Although the cost of drilling a horizontal well with a length of 4000 was more than $1.2 million, this study still explored the potential performance of the well pattern systems compared to the fractured reservoir and could be considered with the development of horizontal drilling technology. Water or CO_2 was injected at 20 °C and 10 MPa from the injection wellhead and the production mass flow rate was 10 kg/s or 20 kg/s in both EGS and well pattern systems. There was one difference between the models of EGS and well pattern systems that the heat transfer between wells and the surrounding rocks in the well pattern systems was calculated radially as introduced before while the simplified heat flux from the rocks to the wells as shown in Eq. (6) was used in the EGS model [42].

$$q = \frac{-4\pi\lambda_s}{\mathrm{In}\left(\frac{2.3089\alpha_s t}{r^2}\right)}\left(T_f - T_{s,i}\right) \tag{6}$$

where λ_s was the thermal conductivity of the rock, α_s was the thermal diffusivity of the rock, t was the time, r was the wellbore

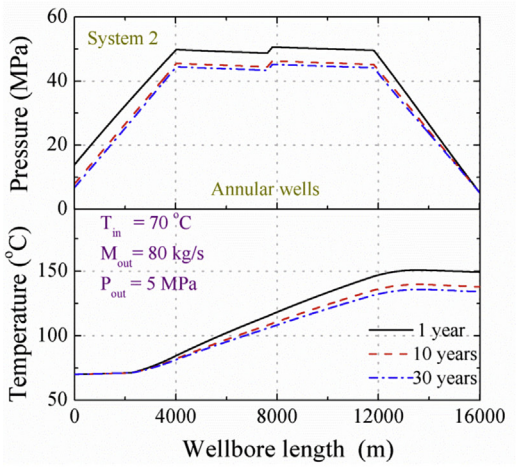

(a) pressure and temperature distributions of water in the tubing along the wellbore length in the annular wells at the operation times of 1 year, 10 years and 30 years

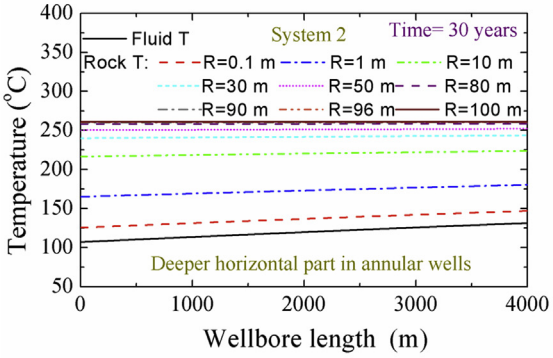

(b) temperature distributions of water in the tubing, rock with a radial distance to the wellbore axis of 0.1 m, 1 m, 10 m, 30 m, 50 m, 80 m, 90 m, 96 m and 100 m along the wellbore length in the deeper horizontal part of the annular wells at the operation time of 30 years

Fig. 5. Temperature and pressure distributions along the wellbore length with the injection temperature of 70 °C, production flow rate of 80 kg/s and production pressure of 5 MPa in annular-wells system.

radius, T_f was the fluid temperature in the wells and $T_{s,i}$ was the initial temperature of the surrounding rock.

Fig. 8 shows the variations of temperatures at the bottomhole and wellhead of the production well with time for different systems with water or CO_2 as the working fluid. After the steady operation of 20 years with the output mass flow rate of 10 kg/s, the systems with the bottomhole temperature of the production well from high to low were eight horizontal wells system with CO_2 as the working fluid, eight horizontal wells system with water as the working fluid, fractured reservoir system with CO_2 as the working fluid, one horizontal well system with CO_2 as the working fluid and one horizontal well system with water as the working fluid, and the bottomhole temperatures of the production well of these systems were respectively 149.5 °C, 145.6 °C, 136.5 °C, 117.0 °C and 69.3 °C (Fig. 8 (a)). The differences between these bottomhole temperatures of the production well indicated the different performances between fractured reservoir, one horizontal well and eight horizontal wells due to the same depth and diameter of the injection well in three systems. Although the bottomhole temperature of the production well in the system with one horizontal well with CO_2 was 19.5 °C lower than that in the system with a fractured reservoir, the system with eight horizontal wells with CO_2 showed a better performance due to the flow distribution, having a production bottomhole temperature of 13.0 °C higher than that in the system with a fractured reservoir.

When it comes to the production wellhead temperature after 20 years with the output mass flow rate of 10 kg/s, the systems with performances from high to low were eight horizontal wells system with water as the working fluid, fractured reservoir system with CO_2 as the working fluid, eight horizontal wells system with CO_2 as the working fluid, one horizontal well system with water as the working fluid and one horizontal well system with CO_2 as the working fluid, and the production wellhead temperatures of these systems were respectively 122.2 °C, 96.5 °C, 73.7 °C, 70.2 °C and

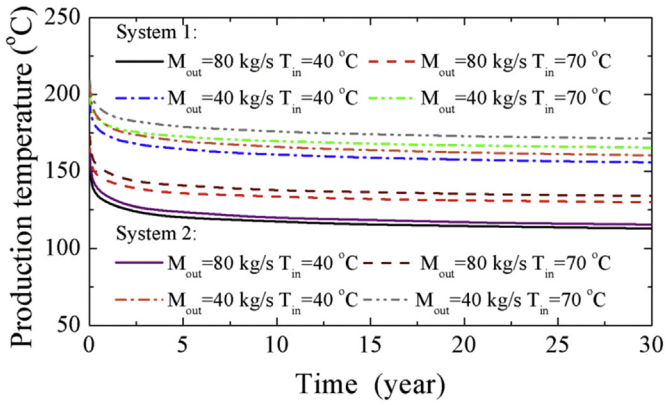

Fig. 6. Variation of production temperature at the production wellhead with time in system 1 and system 2 with different outlet mass flow rates and injection temperatures.

deeper part and the weak expansion of water. However, the large compressibility of CO_2 led to significant expansion along the production well when the pressure decreased, resulting in a pronounced temperature reduction of CO_2 along the production well. For instance, the temperature reduced by 52.5 °C, from 117.0 °C to 64.5 °C, along the production well for one horizontal well system with CO_2. For eight horizontal wells system with CO_2, the temperature decreased by 75.8 °C, from 149.5 °C to 73.7 °C, and this larger temperature decrease compared to one horizontal well system was attributed to the higher production bottomhole temperature which led to more significant heat loss to the surrounding rocks and larger compressibility of CO_2.

For the scenarios with the output mass flow rate of 20 kg/s as shown in Fig. 8 (b), the system with a fractured reservoir underwent the thermal breakthrough and the production bottomhole temperature decreased to 93.6 °C after 20 years. The one horizontal well system with CO_2 had a similar production bottomhole tem-

Table 1
Injection parameters, production parameters, net power, thermal efficiency and working fluid for ORC of water-based geothermal well pattern systems. (time = 30 years, system 1: multi-horizontal-wells, system 2: annular-wells).

System	Production flow rate (kg/s)	Injection temperature (°C)	Injection pressure (MPa)	Production temperature (°C)	Production pressure (MPa)
1	80	40	6.8	113.0	5
	80	70	6.7	130.0	5
	40	40	2.8	155.9	5
	40	70	2.9	165.5	5
2	80	40	8.0	115.8	5
	80	70	7.9	134.1	5
	40	40	3.0	160.4	5
	40	70	3.1	172.0	5

Table 2
Geological conditions of the EGS site at Groβ Schonebekc and characteristic parameters of geothermal systems for comparison [42].

Parameter	Value
Geothermal gradient (°C/m)	0.035
Temperature of ground surface, depth of 4050 m and 4250 m (°C)	8, 149.75, 156.75
Reservoir rock density	2650 kg/m^3
Reservoir rock thermal conductivity	2.9 W/m K
Reservoir rock specific heat capacity	905.7 J/kg K
Injection/production well length (m)	4250
Injection/production wellbore diameter (mm)	230
Distance between injection/production wells for fractured reservoir (m)	424.2
Length of single horizontal well for well pattern systems (m)	4000
Injection temperature (°C)	20
Injection pressure (MPa)	10
Production mass flow rate (kg/s)	10, 20

64.5 °C (Fig. 8 (b)). It could be found that the performances of CO_2 and water were very different in the production well because of the different thermal properties. In the injection well, fluid temperature increased due to the heat extraction from the surrounding rocks, the potential energy loss and its compressibility when the pressure increased [19,45]. Correspondingly, fluid temperature changed along the production well due to the heat exchange with the surrounding rocks, the potential energy increase and its expansion when the pressure decreased. Water had a relatively small compressibility, so the production wellhead temperature was only 23.4 °C lower than the production bottomhole temperature for the system with eight horizontal wells with water as the working fluid. For the system with one horizontal well with water, the temperature increased from 69.3 °C to 70.2 °C along the production well due to the heat extraction from the surrounding rocks in perature with the fractured reservoir, only 2.0 °C lower. Eight horizontal wells systems with CO_2 and with water were still the top two systems according to the underground heat extraction performances. On the other hand, all well pattern systems (with one or eight horizontal wells, with water or CO_2 as the working fluid) had higher production wellhead temperatures compared to the system with a fractured reservoir with CO_2 after 20 years. It was interesting that the production wellhead temperature of one horizontal well system with CO_2 was 53.4 °C, 2.1 °C higher than that of one horizontal well system with water (Fig. 8 (b)). This phenomenon was opposite to the scenario with the output flow rate of 10 kg/s where water showed higher production temperature. This was because the larger mass flow rate caused lower production bottomhole temperature, resulting in a smaller compressibility of CO_2 and a smaller expansion effect of CO_2 along the production well which led

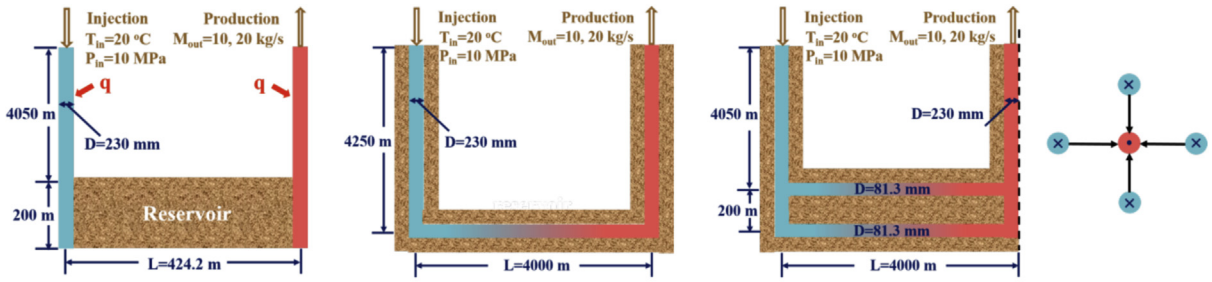

(a) one injection well, one production well and one fractured reservoir [42]

(b) one injection well, one production well and one horizontal well

(c) four injection wells, one production well and eight horizontal wells

Fig. 7. Schematic diagram of three schemes for geothermal energy exploitation for the site at Groβ Schonebekc, Germany.

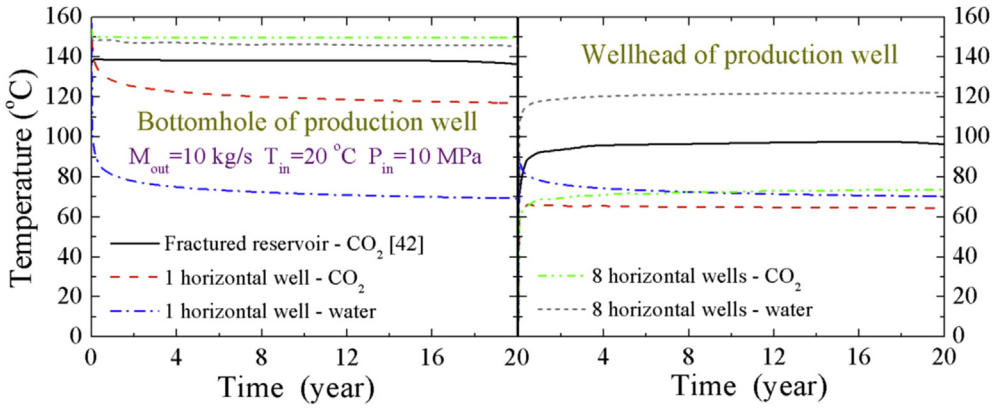

(a) M_{out}=10 kg/s

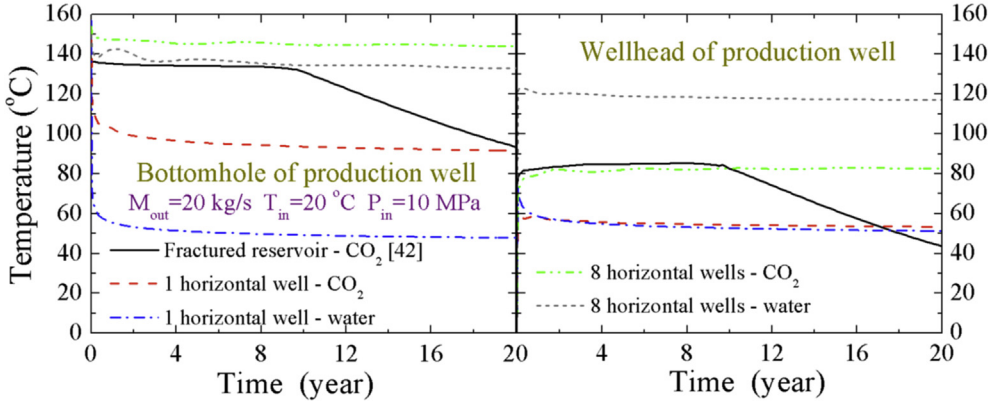

(b) M_{out}=20 kg/s

Fig. 8. Variations of temperatures at the bottomhole and wellhead of the production well with time within 20 years for different systems with water or CO_2 as the working fluid.

to a higher production temperature than water. This gave a direction that CO_2 was more suitable for lower temperature scenarios (lower reservoir temperature or higher output mass flow rate).

For the ground generation system with CO_2 as the working fluid, CO_2 directly flowed into the turbine to do work after the production wellhead, and the production wellhead pressure of CO_2 was an important parameter influencing the net power and the generation efficiency. As shown in Table 3, the production pressure of eight horizontal wells system with CO_2 was higher than that in the EGS with CO_2 due to the smaller pressure loss in the wellbore than in

Table 3
Injection parameters and production parameters of EGS and eight horizontal wells system with CO_2 or water as the working fluid (time = 20 years).

System	Production flow rate (kg/s)	Injection temperature (°C)	Injection pressure (MPa)	Production temperature (°C)	Production pressure (MPa)
Fractured reservoir system with CO_2 [42]	10	20	10	96.5	18.0
	20	20	10	43.8	9.3
8 horizontal wells–CO_2	10	20	10	73.7	19.1
	20	20	10	82.7	20.2
8 horizontal wells-water	10	20	10	122.2	12.6
	20	20	10	117.0	11.8

the porous media. For example, the production pressure was 20.2 MPa with an injection pressure of 10 MPa and flow rate of 20 kg/s in the eight horizontal wells system with CO_2, 10.9 MPa larger than that in fractured reservoir system with CO_2 with the same injection parameters. This higher production pressure was an important advantage of the well pattern systems compared with EGS. It could also be found from Table 3 that although the eight horizontal wells system with water had higher production temperature than that with CO_2, the production pressure of system with CO_2 was much higher than that with water, showing a beneficial effect of CO_2 system to increase the generation efficiency.

5. Conclusions

Novel underground well pattern systems, replacing fracturing reservoir with horizontal wells, were proposed for geothermal energy exploitation in this paper. The most important feature of the well pattern systems was the wholly closed circulation inside the wellbores. Compared to the fractured reservoir system where the fluid flowed in the porous media without a certain flow channel, the closed circulation of the well pattern systems prevented the direct contact, thus the chemical reaction, between the working fluid and the rock surface. Therefore, scaling problem, which was severe in the fractured reservoir system (e.g., in Hijiori project), was unlikely to occur in the well pattern systems. Moreover, the closed circulation inside the wellbores of the well pattern systems ensured the certain flow direction and overcame the problem of mass flow rate loss which was likely to occur in the fractured reservoir system (e.g., mass flow rate loss was as high as 37.5% in Rosemanowes project and 45% in Hijiori project).

A numerical model of the proposed well pattern systems was setup to quantitatively analyze the potential of these systems. Among all the scenarios for both multi-horizontal-wells and annular-wells systems, the scenario with smaller production flow rate of 40 kg/s and larger injection temperature of 70 °C had the largest production temperature. The injection pressure could be lower than the production pressure at smaller production flow rate, thus providing with the self-driven force for the consistent circulation and significantly increasing the generating efficiency. Results also showed that the system with CO_2 as the working fluid had lower production temperature but higher production pressure than the system with water as the working fluid at the same injection temperature, injection pressure and production mass flow rate.

Compared with the system with a fractured reservoir which had a length of 424.2 m, eight horizontal wells system with each horizontal well of 4000 m length had higher production bottomhole temperature. At larger mass flow rate of 20 kg/s, the injection temperature of 20 °C and the injection pressure of 10 MPa, the production wellhead temperature of eight horizontal wells system with CO_2 as the working fluid was 38.9 °C higher than that in fractured reservoir system with CO_2 after 20 years, showing a significant application potential. At the injection temperature of 20 °C and the injection pressure of 10 MPa, the production wellhead pressure of eight horizontal wells system with CO_2 as the working fluid was respectively 1.1 MPa and 10.9 MPa larger than that in the fractured reservoir system with the production mass flow rate of 10 kg/s and 20 kg/s. The larger production wellhead pressure of the well pattern system, as another advantage, was caused by the smaller pressure drop in the wellbore compared to that in the porous media (reservoir rock) and was beneficial for power generation.

Acknowledgments

This project was supported by the National Natural Science Foundation of China (No. 51536004), the Innovative Research Groups of the National Natural Science Foundation of China (No. 51321002), the Research Project of Chinese Ministry of Education (No. 113008A), and Beijing Key Laboratory Development Project (Z151100001615006).

References

[1] IEA, Technology Roadmap: Geothermal Heat and Power, OECD/IEA, 2011.
[2] J.W. Tester, B.J. Anderson, A.S. Batchelor, D.D. Blackwell, R. DiPippo, E.M. Drake, J. Garnish, B. Livesay, M.C. Moore, K. Nichols, S. Petty, M.N. Toksoz, R.W. Veatch Jr., The Future of Geothermal Energy: Impact of Enhanced Geothermal Systems (EGS) on the United States in the 21st Century, DOE Contract DE-AC07–05ID14517 Final Report, Massachusetts Institute of Technology, 2006.
[3] W. Moomaw, P. Burgherr, G. Heath, M. Lenzen, J. Nyboer, A. Verbruggen, Annex II: methodology, in: IPCC Special Report on Renewable Energy Sources and Climate Change Mitigation, 2011.
[4] R.N. Xu, L. Zhang, F.Z. Zhang, P.X. Jiang, A Review on heat transfer and energy conversion in the enhanced geothermal systems with water/CO_2 as working fluid, Int. J. Energy Res. 39 (13) (2015) 1722–1741.
[5] Australian Renewable Energy Agency, Looking Forward: Barriers, Risks and Rewards of the Australian Geothermal Sector to 2020 and 2030, 2014.
[6] M.Y. Li, N. Lior, Analysis of hydraulic fracturing and reservoir performance in enhanced geothermal systems, J. Energy Resour. Tech.-Trans. ASME 137 (4) (2015), 041203.
[7] M.Y. Li, N. Lior, Comparative analysis of power plant options for enhanced geothermal systems (EGS), Energies 7 (12) (2014) 8427–8445.
[8] J.L. Chen, F.M. Jiang, Designing multi-well layout for enhanced geothermal systems to better exploit hot dry rock geothermal energy, Renew. Energy 74 (2015) 37–48.
[9] T.C. Ekneligoda, K.-B. Min, Determination of optimum parameters of doublet system in a horizontally fractured geothermal reservoir, Renew. Energy 65 (2014) 152–160.
[10] T.C. Ekneligoda, K.-B. Min, Determination of optimum parameters of doublet system in a horizontally fractured geothermal reservoir, Renew. Energy 65 (2014) 152–160.
[11] F.Z. Zhang, P.X. Jiang, R.N. Xu, System thermodynamic performance comparison of CO_2-EGS and water-EGS systems, Appl. Therm. Eng. 61 (2013) 236–244.
[12] C. Alimonti, E. Soldo, Study of geothermal power generation from a very deep oil well with a wellbore heat exchanger, Renew. Energy 86 (2016) 292–301.
[13] A. Galgaroa, Z. Farinaa, G. Emmib, M.D. Carlib, Feasibility analysis of a borehole heat exchanger (BHE) array to be installed in high geothermal flux area: the case of the Euganean thermal basin, Italy, Renew. Energy 78 (2015) 93–104.
[14] P.J. Yekoladio, T. Bello-Ochende, J.P. Meyer, Design and optimization of a downhole coaxial heat exchanger for an enhanced geothermal systems (EGS), Renew. Energy 55 (2013) 128–137.
[15] S.E. Dehkordi, R.A. Schincariol, S. Reitsma, Thermal performance of a tight borehole heat exchanger, Renew. Energy 83 (2015) 698–704.
[16] S. Finsterle, Y.Q. Zhang, L.H. Pan, P. Dobson, K. Oglesby, Microhole arrays for improved heat mining from enhanced geothermal systems, Geothermics 47

(2013) 104–115.
[17] R. Jeanloz, H.A. Stone, JASON review of enhanced geothermal systems, in: Proceedings, Thirty-ninth Workshop on Geothermal Reservoir Engineering Stanford University, Stanford, California, February 24-26, 2014.
[18] H. Wolff, S. Schmid, Geothermal electricity generation project - underground closed geothermal heat exchanger, in: Symposium: Geothermal Electricity – an Investment in the Future, June 20-21, 2002.
[19] P.X. Jiang, X.L. Li, R.N. Xu, Y.S. Wang, M.S. Chen, H.M. Wang, B.L. Ruan, Thermal modeling of CO_2 in the injection well and reservoir at the ordos CCS demonstration project, China, Int. J. Greenh. Gas Control 23 (2014) 135–146.
[20] C. Vincent, S.F. Dai, W.Y. Chen, R.S. Zeng, G.S. Ding, R.N. Xu, T. Vangkilde-Pedersen, F. Dalhoff, Carbon dioxide storage options for the COACH project in the Bohai Basin, China, Energy Procedia 1 (2009) 2785–2792.
[21] F. Yang, B. Bai, S. Dunn-Norman, R. Nygaard, A. Eckert, Factors affecting CO_2 storage capacity and efficiency with water withdrawal in shallow saline aquifers, Environ. Earth Sci. 71 (2014) 267–275.
[22] F. Luo, R.N. Xu, P.X. Jiang, Numerical investigation of the influence of vertical permeability heterogeneity in stratified formation and of injection/production well perforation placement on CO_2 geological storage with enhanced CH_4 recovery, Appl. Energy 102 (2013) 1314–1323.
[23] K. Pruess, Enhanced geothermal systems (EGS) using CO_2 as working fluid – a novel approach for generating renewable energy with simultaneous sequestration of carbon, Geothermics 35 (2006) 351–367.
[24] J. Finger, R. Jacobson, C. Hickox, J. Combs, G. Polk, C. Goranson, Slimhole Handbook: Procedures and Recommendations for Slimhole Drilling and Testing in Geothermal Exploration, Sandia National Laboratories, Albuquerque, New Mexico, USA, 1999, p. 164. Report SAND99-1076.
[25] S.D. Joshi, Horizontal Wells: Successes and Failures, Petroleum Society of Canada, 1994, http://dx.doi.org/10.2118/94-03-01.
[26] http://www.guinnessworldrecords.com/world-records/longest-drilled-oil-well/.
[27] PH. Moe, KM. Rabben, Plant for exploiting geothermal energy: U.S. Patent 6,247,313, 2001-6-19.
[28] S.K. Garg, J. Combs, A Study of Production/Injection Data from Slim Holes and Large-diameter Wells at the Okuaizu Geothermal Field, Tohoku, Japan, Idaho National Engineering and Environmental Laboratory, Idaho, USA, 2002, p. 257. Report INEEL/EXT-02-01429.
[29] S.K. Sanyal, S.J. Butler, An analysis of power generation prospects from enhanced geothermal systems, Trans. Geotherm. Resour. Counc. 29 (2005) 131–138.
[30] RM. Potter, JW. Tester. Continuous drilling of vertical boreholes by thermal processes: including rock spallation and fusion. Patent publication date: 30 June 1998.
[31] RS. Polizzotti, LL. Hirsch, AB. Herhold, MD. Ertas. Hydrothermal drilling method and system. Patent publication date: 3 July 2003.
[32] H.B. Curlett, C.J. Geddes, Leveraging a new energy source to enhance heavy oil and oil sands production, GRC Bull. 35 (2006) 32–36.
[33] R.N. Xu, F. Luo, P.X. Jiang, Experimental research on the turbulent convection heat transfer of supercritical pressure CO_2 in a serpentine vertical mini tube, Int. J. Heat Mass Transf. 91 (2015) 552–561.
[34] X.Y. Liu, J. Zhao, C. Shi, B. Zhao, Study on soil layer of constant temperature, Acta Energiae Solaris Sin. 28 (5) (2007) 494–498.
[35] SPT Group, OLGA 7 User Manual, 2010.
[36] X.L. Li, R.N. Xu, L.L. Wei, P.X. Jiang, Modeling of wellbore dynamics of a CO_2 injector during transient well shut-in and start-up operations, Int. J. Greenh. Gas Control 42 (2015) 602–614.
[37] K.H. Bendlksen, D. Maine, R. Moe, S. Nuland, The Dynamic Two-fluid Model OLGA: Theory and Application, SPE Production Engineering, 1991, p. 19451.
[38] R. Span, W. Wagner, A new equation of state for carbon dioxide covering the fluid region from the triple-point temperature to 1100 K at pressures up to 800 MPa, J. Phys. Chem. Ref. Data 25 (1996) 1509–1596.
[39] K.S. Pedersen, A. Fredenslund, P. Thomassen, Properties of Oils and Natural Gases, Gulf Publishing Company, Houston, Texas, 1989.
[40] J.R. Cooper, R.B. Dooley, Revised Release on the IAPWS Industrial Formulation 1997 for the Thermodynamic Properties of Water and Steam, The International Association for the Properties of Water and Steam, Lucerne, Switzerland, August 2007.
[41] A.R. Hasan, C.S. Kabir, Fluid Flow and Heat Transfer in Wellbores, SPE Richardson, Texas, 2002.
[42] F. Luo, R.N. Xu, P.X. Jiang, Numerical investigation of the doublet enhanced geothermal system with CO_2 as working fluid (CO_2-EGS), Energy 64 (2014) 307–322.
[43] M.G. Blocher, G. Zimmermann, I. Moeck, W. Brandt, A. Hassanzadegan, F. Magri, 3D numerical modeling of hydrothermal processes during the lifetime of a deep geothermal reservoir, Geofluids 10 (2010) 406–421.
[44] W.E. Hefley, et al., The Economic Impact of the Value Chain of a Marcellus Shale Well, Working Paper, Katz Graduate School of Business, Katz Graduate School of Business, University of Pittsburgh, Pittsburgh, PA, 2011.
[45] B.L. Ruan, R.N. Xu, L.L. Wei, X.L. Ouyang, F. Luo, P.X. Jiang, Flow and thermal modeling of CO_2 in injection well during geological sequestration, Int. J. Greenh. Gas Control 19 (2013) 271–280.